Journal of Materials Chemistry C

PAPER

View Article Online
View Journal | View Issue

Cite this: J. Mater. Chem. C, 2016, 4, 10061

Environment-friendly carbon nanotube based flexible electronics for noninvasive and wearable healthcare†

Toan Dinh,*[a] Hoang-Phuong Phan,[a] Tuan-Khoa Nguyen,[a] Afzaal Qamar,[a] Abu Riduan Md Foisal,[a] Thanh Nguyen Viet,[b] Canh-Dung Tran,[c] Yong Zhu,[ad] Nam-Trung Nguyen[a] and Dzung Viet Dao[ad]

Received 30th June 2016,
Accepted 29th September 2016

DOI: 10.1039/c6tc02708c

www.rsc.org/MaterialsC

Flexible and stretchable electronics have a wide variety of wearable applications in portable sensors, flexible electrodes/heaters, flexible circuits and stretchable displays. Spinnable carbon nanotubes (CNTs) constructed on flexible substrates are potential materials for wearable sensing applications owing to their high thermal and electrical conductivity, low mass density and excellent mechanical properties. Here, we demonstrate a wearable thermal flow sensor for healthcare using lightweight, high strength, flexible CNT yarns as hotwires, pencil graphite as electrodes, and lightweight, recyclable and biodegradable paper as flexible substrates, without using any toxic chemicals. The CNT-based sensor which could be utilized to monitor respiratory diseases is comfortably affixed to human skin and detects real-time human respiration. We also successfully demonstrate the temperature detecting functionality integrated in the same sensor, which can measure body temperature using a non-contact mode. The results indicate that the CNT yarn can be used to develop a wide range of environment-friendly, low-cost and lightweight paper-based flexible devices for wearable applications in temperature and respiratory monitoring, and personal healthcare.

1 Introduction

The development of conventional electronics has been driven towards high sensitivity, durability, miniaturization and integration abilities.[1–4] These devices found applications in harsh environments such as high temperatures and corrosion.[5,6] However, for human-activity monitoring and personal healthcare, an alternative approach is required to develop a new generation of wearable electronics for the emerging demand, which not only focuses on achieving high sensitivity, but also on the flexibility, stretchability and suitability for human services.[7–12] Wearable and flexible devices, which can be embedded in clothes or affixed to human skin, are obviously of interest for those applications in personal healthcare and therapeutics.[9,13–15] For instance, there has recently been significant progress in the achievement of wearable physical sensors which enable the monitoring of body temperature, body motion, muscle movement, heart rate and voice.[16–18] Because of the difficulties in establishing new flexible/stretchable structural platforms from conventional brittle materials (*e.g.* silicon and diamond), the mainstream strategy to achieve wearable electronics relies on the fabrication of stretchable functional materials or stretchable structures on a flexible and stretchable substrate.[19–21] As such, advanced nanomaterials including carbon nanotubes, silver nanowires, graphene and hybrid materials have been constructed on polydimethylsiloxane (PDMS) and polyethylene naphthalate (PEN) to make flexible, stretchable and multifunctional electronic devices for wearable applications.[21–23] The successful fabrication of these devices indicates a promising future for flexible and stretchable electronics facilitating personal healthcare.

Recent research studies on carbon nanotube (CNT) based flexible and stretchable electronic devices have demonstrated numerous successful applications such as transparent, flexible and stretchable diodes,[24] transistors,[25] strain sensors[26] and flexible displays,[27] owing to the high intrinsic carrier mobility, excellent conductivity, and mechanical flexibility of CNTs. To date, enormous progress in the development of CNT based devices has been made thanks to the significant improvement in the electrical properties and mechanical properties of CNTs.[28–31] The successful demonstration of these CNT-based

[a] Queensland Micro- and Nanotechnology Centre, Griffith University, Queensland, Australia. E-mail: toan.dinh@griffithuni.edu.au
[b] School of Transportation Engineering, Hanoi University of Science and Technology, Hanoi, Vietnam
[c] School of Mechanical and Electrical Engineering, University of Southern Queensland, Queensland, Australia
[d] School of Engineering, Griffith University, Queensland, Australia

† Electronic supplementary information (ESI) available. See DOI: 10.1039/c6tc02708c

devices indicates that there is a huge demand for low-cost, environment-friendly and wearable electronics using these advanced materials. Furthermore, strategies to achieve the flexibility and stretchability of CNT-based devices have commonly relied on their construction on plastic,[32] polyester (PE),[26] polyethylene terephthalate (PET), glass, polymethyl-methacrylate (PMMA) and polydimethylsiloxane (PDMS).[33] However, these materials are of heavy weight and are non-biodegradable. Additionally, the fabrication of CNT based flexible devices using these substrates typically requires additional toxic solvents such as thionyl chloride and polyamic acid,[24,32] which are unfriendly for both the user and the environment. The solvent-involving processes could also lead to various environmental contamination issues. Moreover, additional complex steps have been involved in the fabrication of flexible and stretchable CNT-based electronic devices, namely the dispersion of CNTs in a specific solvent, employing magnetic stirring or ultrasonication.[35–37] These advanced steps have made their fabrication more challenging, sophisticated and time-consuming. Therefore, there is a great need to develop the next generation of user-friendly, environment-friendly flexible and stretchable electronic devices for monitoring human health and other wearable applications.

Here, we have developed an inexpensive, eco-friendly and lightweight wearable thermal flow sensor for the noninvasive monitoring of human respiration, integrated with temperature-sensing functionality. The hot wire flow sensor is fabricated using a solvent-free and lightweight CNT yarn, as well as graphite pencil shading as an electrode, on low-cost, lightweight, recyclable and biodegradable cellulose papers without using any toxic solvents or hazardous chemicals. The temperature-dependent electrical properties of CNT yarns are investigated and the conduction mechanism is discussed. We have found a relatively large negative temperature coefficient of resistance (TCR) and fast thermal response, which are utilized to develop a wearable flow-monitoring device. This device can also serve as a temperature sensing element. With their fiber geometry, mechanical flexibility and being lightweight, the all-carbon thermal flow sensors hold tremendous prospects for low cost, eco-friendly and multi-functional wearable applications, including respiratory monitoring in personal healthcare.

2 Materials and fabrication

Fig. 1a shows the scanning electron microscopy (SEM) image of a CNT yarn with a diameter of 12 μm and Young's modulus of approximately 1.2 GPa. The detailed fabrication process for CNT yarns has been reported by Tran *et al.*[28] The brief process is presented in Fig. S1, ESI.† Fig. 1b shows the SEM image of the paper substrate which reveals a randomly oriented network of cellulose fibers and also the porosity of the paper. Fig. 1c schematically illustrates a CNT yarn device constructed on a cellulose paper substrate with a bridge-island configuration, which consists of two spatially isolated graphite electrodes (blue squares) electrically connected by a unstrained CNT yarn bridge (red wire). Electrical interconnection was established using conductive paste (not shown here). Different from the fabrication methods for CNT-based flexible and stretchable devices reported in the literature,[24,32,35–37] our approach is friendly for both the user and the environment because it involves cost-effective, lightweight, environment-friendly materials, without using any solvents or toxic chemicals. In addition, this strategy enables the strip to be bent, twisted and folded without damaging the CNT wire under bending or torsional conditions. Fig. 1d indicates that the as-fabricated device is mechanically bendable, flexible and hence, wearable. We tested the device

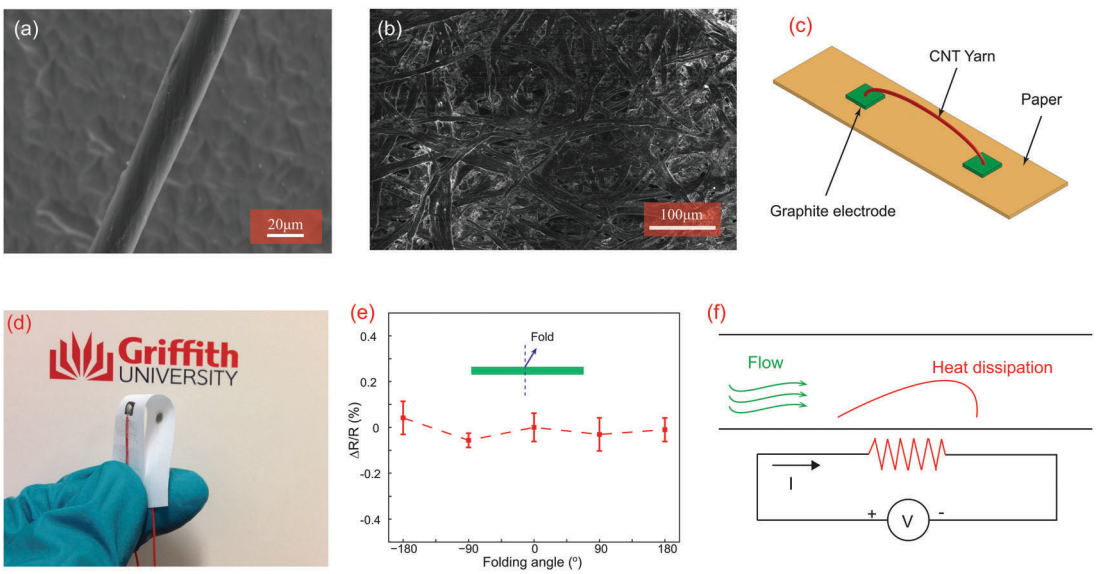

Fig. 1 CNT yarns and fabrication of flexible devices. (a) A scanning electron microscope (SEM) image of a CNT yarn. (b) A SEM image of the cellulose fiber paper. (c) Schematic sketch of a CNT-based flexible device. (d) Photograph of the device showing its flexibility. (e) Relative resistance change of the device folded under various curvature angles. (f) Schematic illustration of the working principle of the thermal flow sensor.

with different folding angles, Fig. 1e. Various folding tests showed a maximum resistance change of approximately 0.2% which indicates the good stability of the CNT yarn based device. This stability is attributed to the fact that the pure CNT yarns have a negligible electrical resistance change under applied strain/stress[38,39] with a very small gauge factor of approximately 0.5, which is at least four times lower than that of metals. Also, due to the unstrained state of the CNT yarns, the bending and torsion of the paper substrate induce a negligible stress/strain on the yarns.

Fig. 1f shows the principle of the as-fabricated CNT based device for airflow monitoring. The CNT hotwire flow sensor operates under the convective heat transfer between a hot wire and the surrounding environment.[34,40,41] When a current or voltage is applied to a CNT hotwire, its temperature rises due to the Joule heating effect. As airflow passes around the hot wire, its resistance increases, owing to the negative TCR of the CNT yarn, the result of which will be presented hereafter. By acquiring this change, the airflow velocity is measured.

3 Temperature sensors

In our work, the thermosensitivity of the CNT-based thermistor was studied by examining the electrical resistance change at different temperatures. Typically, the thermistor was configured as a resistance temperature detector (RTD). Because the application of the as-fabricated CNT flexible temperature sensors is intended for body health monitoring and human skin, the working temperature ranges are commonly lower than 80 °C. Fig. 2a shows the typical current–voltage (I–V) curves of the RTD at various temperatures when the applied voltages vary from −0.2 V to +0.2 V. The linear I–V characteristics indicate a good Ohmic contact between the graphite electrodes and the CNT yarn. The normalized resistance change $[\Delta R/R = (R - R_0)/R_0]$ was measured, where R_0 and R are the resistances at room temperature (25 ± 2 °C) and elevated temperatures, respectively. Fig. 2b shows that the resistance of the CNT yarn decreased as the temperature increased. This indicates that the conduction of the CNT yarn is thermally activated with increasing temperature, corresponding to a negative temperature coefficient of resistance (TCR). When temperature increases, there is a decrease in the carrier mobility due to scattering effects,[42,43] which can lead to a decrease in electrical conductivity. However, increasing temperature also results in an increase in the number of carriers of individual CNTs, which are excited by thermal energy.[42,43] At temperatures close to 25 °C, it is expected that the impact of generated carriers on the CNT yarn conductivity is more significant than that of

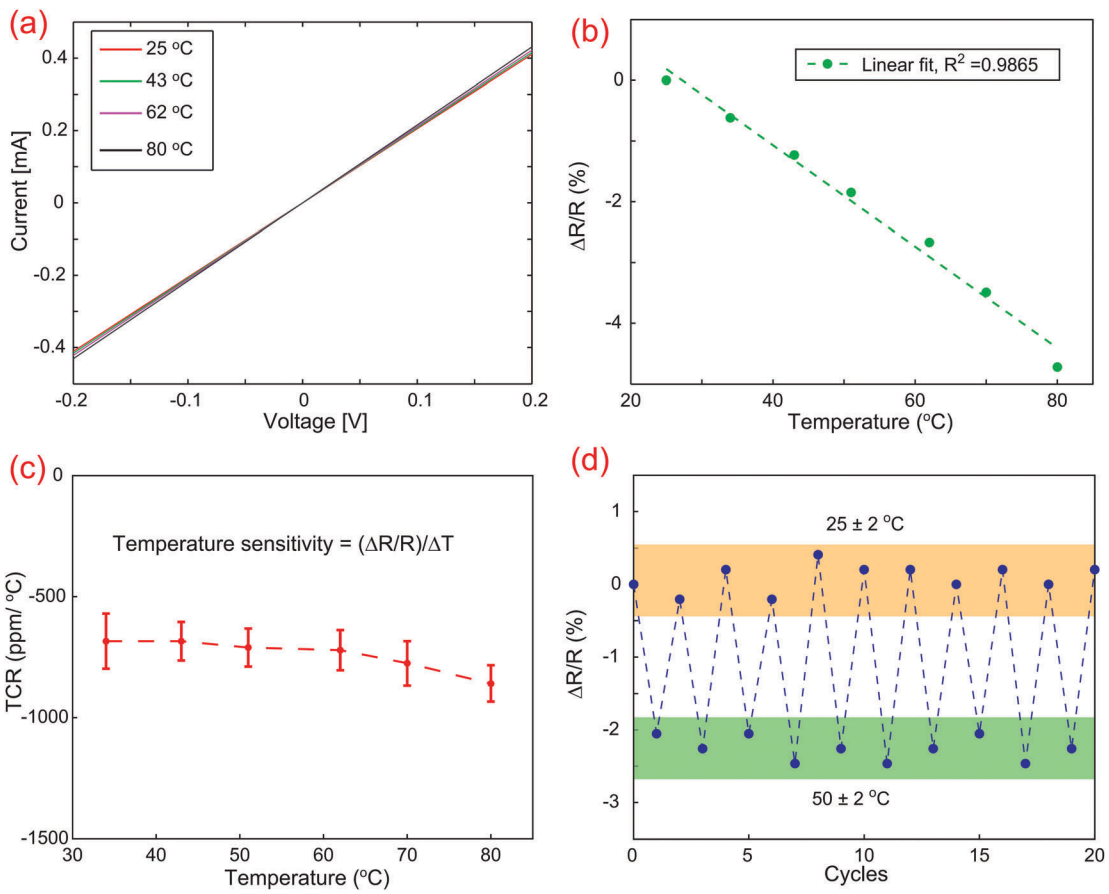

Fig. 2 Temperature sensor. (a) I–V characteristics of the CNT-based thermistor at different temperatures. (b) Normalized resistance changes of the temperature sensor *versus* temperature. (c) Temperature coefficient of resistance (temperature sensitivity) of the CNT-based temperature sensor. (d) Cyclic temperature tests of the CNT-based sensor between room temperature and 50 °C, which indicate good repeatability.

the scattering effect. Therefore, the resistance of the CNT yarn decreases with increasing temperature. In addition, as the CNTs are twisted together, we hypothesise that the contact area between adjacent single CNTs could increase with increasing temperature, due to the expansion of individual CNTs. This leads to a decrease in contact resistance between the adjacent CNTs. Therefore, the overall decrease in electrical resistance of the CNT yarn will be more significant with the contribution of contact resistance improvement. In other words, the temperature sensitivity decreases with increasing temperature. However, it is worth noting that this variation is small with increasing temperature, as shown in Fig. 2c. Therefore, if the temperature effect on the contact resistance between the single CNTs is neglected, the single CNT and the CNT yarn could show a similar temperature dependence of electrical resistance. In addition, the TCR or the temperature sensitivity of the sensors is calculated using [TCR = $\Delta R/R \times 1/\Delta T$]. Fig. 2c shows a relatively stable, large and negative TCR which is approximately 750 ppm K^{-1}. This temperature sensitivity is comparable to that of other flexible and stretchable temperature sensors reported in the literature which have been fabricated involving toxic solvents and complex fabrication steps.[44,45] It is also worth noting that the TCR of the CNT yarn was found to be comparable to that of single-walled (SWCNT) and multi-walled (MWCNT) carbon nanotubes which have been utilized as small-size and sensitive temperature sensors.[46,47] This indicates that the temperature effect on the electrical contact between the single CNTs in the CNT yarns is negligible. Therefore, the temperature sensitivity of the flexible CNT yarn sensors can be calculated, owing to the temperature dependent electrical conductivity of individual CNTs as follows:[38,50]

$$R_{tot} = R_s + \frac{1}{|t|^2}\frac{h}{8e^2}\left[1 + \exp\left(\frac{E_{gap}}{kT}\right)\right] \quad (1)$$

where R_s is the contact resistance between electrodes and the CNT yarn which can be neglected since the electrodes have good contact with the yarn, h and k are Planck's constant and the Boltzmann constant, respectively; e is the electron charge and E_{gap} is the band energy gap. T is the absolute temperature and $|t|^2$ is the transmission probability of the electrons across the band gap barrier. Eqn (1) indicates that the resistance of the CNT is exponentially dependent on the absolute temperature. However, due to the application of the narrow temperature range from 25 °C to 80 °C, the electrical resistance change is almost linear as shown in Fig. 2b.

In addition, due to the fact that the performance of the sensor can be degraded over a period of time, multiple cycle tests of the temperature difference between the room temperature (25 ± 2 °C) and (50 ± 2 °C) were performed to obtain the resistance changes of the sensor. Fig. 2d indicates that the CNT RTD operated consistently in the temperature cycle tests. This also confirms the thermal stability of the flexible temperature sensor, which is an essential characteristic for flexible electrical devices.

Fig. 3a shows the time response of the RTD to the environmental temperature varying from 35 °C to 65 °C, which was established by approaching and moving away from the surface of a hot plate. The hot plate temperature was controlled and monitored using a reference temperature sensor. The as-shown ON–OFF state responses for each of the 4 cycles remained the same, indicating the reversibility and stability of the temperature sensor. We further demonstrated the feasibility of using the RTD for temperature measurement of the human body by approaching and moving away a finger from the CNT wire (without touching). Fig. 3b shows the response of the sensor to the temperature of the finger with three approaching-withdrawing times. When the finger approached, the temperature surrounding the CNT wire increased, leading to a decrease in its electrical resistance. It is worth noting that unlike bulky temperature sensors, the CNT yarn based RTD is small in size (a diameter of 12 μm); therefore it has a fast response to environmental temperature change and it is also easy to get uniform temperature distribution. This good performance can be achieved thanks to the small size of the CNT hotwire[48] and the thermal properties of the wire and the paper substrate. The thermal conductivity of the paper is relatively low, while the thermal conductivity of the CNT is extremely large[49] with direct contact to the graphite only at the ends. This allows a high thermal transport rate within the yarn, achieving a uniform temperature distribution corresponding

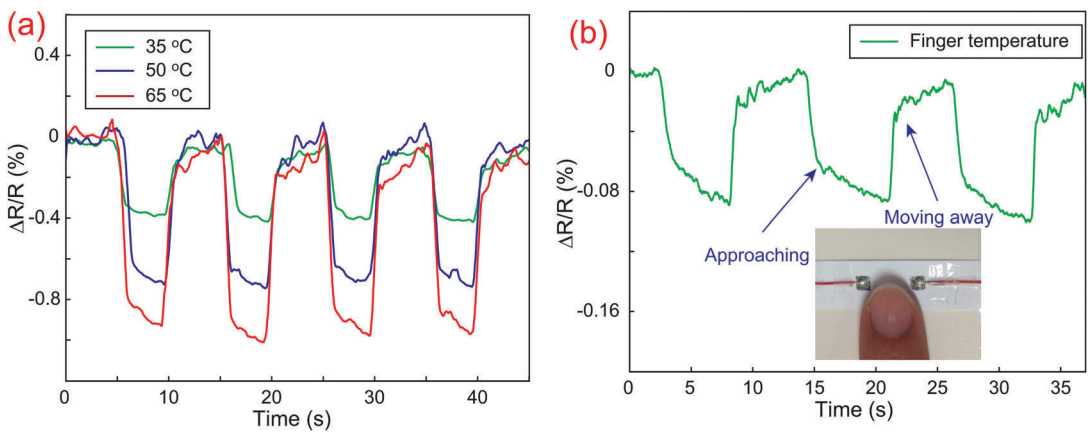

Fig. 3 Temperature detection. (a) Relative resistance change of the device for different temperatures in the heater-on and heater-off states. (b) Thermoresponse of the CNT temperature sensor when the finger approaches and moves away from the sensor.

to a small Biot number. Moreover, because the yarn has a high surface area-to-volume ratio and a very small thermal inertia, the response is very fast to temperature changes of the air surrounding the CNT wire. Consequently, the resistance change was obviously detected. The obtained result indicates that the flexible CNT temperature sensor can be applied to monitor human temperature under real-time conditions.

4 Wearable airflow sensors for noninvasive respiratory monitoring

As presented in the previous section, the CNT wire has a relatively high thermosensitivity; thus it holds great potential for thermal sensing applications. One of these important applications is airflow monitoring which will be demonstrated next.

We investigated the airflow response of the CNT hotwire using the experimental setup shown in Fig. S2, ESI.† Fig. 4a demonstrates the real-time response of the flow sensor under different airflow velocities. It is noteworthy that the relative resistance change of the sensor increases with increasing air flow rates and returns to the initial value when the flow ceases, indicating a good reproducibility of the sensor characteristics. Fig. 4b illustrates the relationship between the airflow velocity ν and the differential output voltage of the sensor ΔU, which can be formulated as $\Delta U = a + b\nu^n$, where a, b and n are experimental constants. As the sensor operated under a constant current of 3 mA, the sensitivity of the thermal flow sensor was found to be 1.208 mV $(\text{m s}^{-1})^{-0.8}$ at a relatively low power consumption of 4.4 mW, which is comparable to that of the platinum thermal flow sensor reported in the literature.[51,52] This result indicates that the CNT yarn flexible hotwire can be used for sensitive flow monitoring. As such, the temperature around the hotwire increased and reached a steady state when a constant current of 3 mA was applied. As airflow passes over the CNT hotwire, convective heat loss increases from the hotwire to the ambient air. Therefore, the temperature of the hotwire decreased and reached a new steady state. The decrease in the temperature of the hotwire leads to a large increase in its electrical resistance, owing to its relatively large negative temperature coefficient of resistance (TCR). As the resistance of the CNT yarn is sensitive to temperature variation, a low airflow rate can be detected. In other words, the hotwire can be utilized for sensitive airflow monitoring. More interestingly, the sensitivity of a thermal flow sensor can increase with a higher applied constant current or power.[34,53] Therefore, the sensitivity of the CNT hotwire can be improved because our experiment has proved that the CNT hotwire is sensitive to airflow changes even at a low power consumption. This low power consumption is attributed to the small size and to the good thermal isolation of the wire fixed on paper and surrounded by air. This enables large thermal gradients near the heater, and hence, a high responsivity to air flow.[54] It is also noteworthy that losses due to conduction and radiation are expected to be very small, owing to the good insulation of the sensors.

For dynamically measuring the airflow changes, a fast response of a thermal flow sensor is desired. Therefore, we measured the time response of a CNT hot wire at different applied currents. As shown in Fig. 4c and d, a very fast response time of approximately 80 ms was found for the CNT hot wire, corresponding to a bandwidth of 12.5 Hz. This bandwidth satisfies the requirement to measure the typical respiratory rate of a patient, which normally

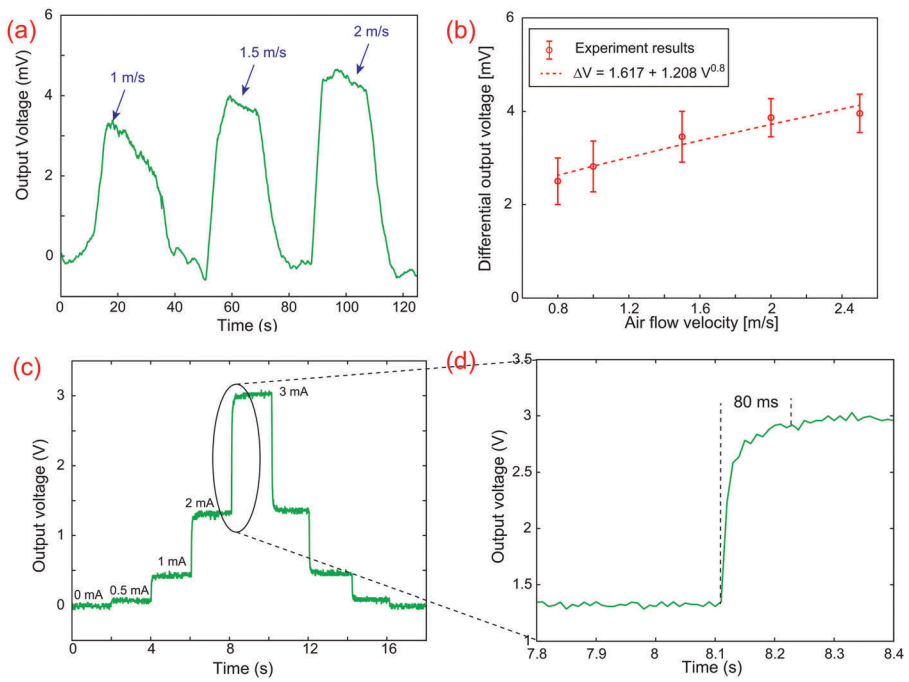

Fig. 4 CNT-based flow sensors. (a) Response of the sensor under different airflow velocities. (b) Differential output voltage. (c and d) Thermal response time of the CNT-based hotwire.

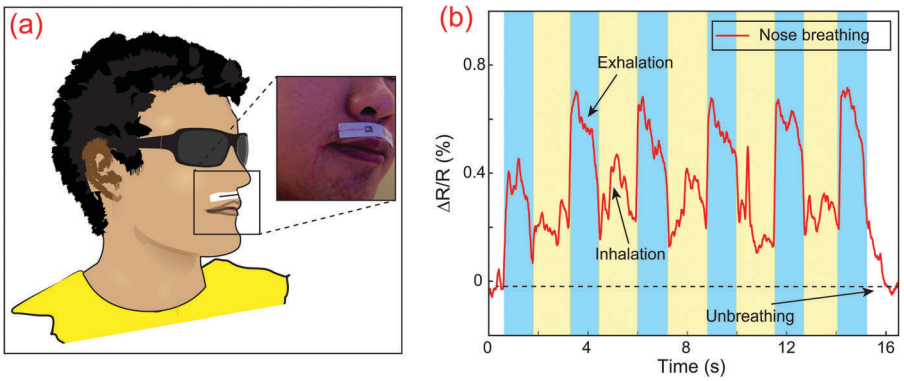

Fig. 5 Noninvasive monitoring of respiratory flow. (a) Photograph of a wearable flow-monitoring device affixed to the human upper lip for respiratory monitoring. (b) Response of the CNT-based wearable thermal flow sensor under nose breathing conditions.

lies between 12 and 20 breaths per minute. The uncertainty of the flow measurement was examined showing that the higher the temperature in the CNT hot wire, the larger the uncertainties (Fig. S3, ESI†).

It is well known that mouth respiration and nose breathing can bring about changes in the airflow rate. Monitoring human respiration is an effective approach which has been utilized for the treatment of respiratory diseases. However, the current systems for respiratory airflow monitoring have commonly involved nasal cannulas, which consist of two small pipes to be invasively inserted into the nostrils.[11,18] This leads to uncomfortable and unsmooth breathing for patients. Therefore, wearable flow sensors have been proven to be effective for noninvasive respiratory monitoring.[11,55,56] We demonstrated the feasibility of using a CNT thermal flow sensor for nose breathing by affixing it to the human upper lip. Thanks to the lightweight and natural flexibility of the sensor made of CNT, graphite and the biodegradable cellulose fiber paper substrate, the CNT paper-based sensor offers wearable functionality and good comfortability for respiratory patients (Fig. 5a). Fig. 5b shows the periodic signal generated by inhalation and exhalation. It is worth mentioning that the exhalation process creates larger changes in the electrical resistance of the sensor. This indicates that in comparison to inhalation, exhalation causes a larger flow rate through the sensor. More interestingly, a CNT-based flow sensor for monitoring mouth respiration was fixed on a table to avoid the effects of agitation. The response of the sensor was measured with a high signal-to-noise ratio, and multiple testes were also conducted, showing good repeatability of signals from the sensor (Fig. S4, ESI†). The results demonstrate that the flexible and wearable CNT flow sensor is capable of monitoring human breath in real time, and can be used for various applications in human medical monitoring, sleep quality perception and other personal healthcare.

5 Conclusion

In conclusion, the results herein demonstrate simple and eco-friendly CNT-based flexible electronics using lightweight, high strength and flexible CNT yarns, which were constructed on low-cost, recyclable and biodegradable printing paper using commercially available pencil graphite shading as electrodes. We successfully demonstrated a CNT-based flexible device as a sensitive wearable thermal flow sensor which can noninvasively monitor human respiration in real time. We also demonstrated the temperature sensing functionality of the device for human-body temperature detection. We believe that the flexible electronics fabricated by this user-friendly and solvent-free method evidence the development of the next generation of eco-friendly, lightweight and wearable devices which can be utilised for applications in respiratory monitoring and other personal healthcare.

6 Experimental section

Fabrication of pure CNT yarns

The CNT yarn was fabricated from spinnable multi-wall CNT yarns spun using a modified process with 8000 turns per meter and a heat treatment of 200 °C.

Fabrication of the CNT yarn based thermal flow sensor

A printing paper (A4, Staples) with a thickness of 110 μm was used as a substrate and a commercial graphite pencil (5B, Faber Castell) was employed to make the electrodes with dimensions of 3 mm × 3 mm. First, the two squared electrodes were formed using the pencil drawing method. In the next step, a pure CNT yarn with a length of 12 mm was placed on the two electrodes. Finally, electrical interconnections were created using a conductive paste (186-3616, RS Components). The fabrication process is shown in Fig. S5, ESI.† The device was then annealed at a temperature of 80 °C for 1 hour to improve the electrical conductivity and stability.

Measurement of temperature and air flow

We conducted the temperature-dependent electrical properties of the CNT yarns in a precise temperature-controlled oven with a reference temperature sensor (K type thermocouple, 0.1 °C resolution). The *I–V* characteristics were measured using a HP 4145B analyser. The thermal response of the CNT yarns to surface temperature was conducted using a hot plate (RT Stirring, ThermoSciencetifics). All real-time responses of the sensor were monitored using a measurement module including a wheatstone bridge connected with an amplifier (AD623AN, Analog Devices)

and an oscilloscope (MSO-X 3104A, Agilent Technologies). We used an air blower (LB0115-002, Industrial Equipment and Control) to generate the different air velocities and a reference hot wire anemometer (AM-4204, RS Components) to measure the airflow rate.

All experiments regarding the measurement of human respiration and sensing of finger's temperature were performed in compliance with the relevant laws and institutional guidelines and approved by the Human Research Ethics Committee (HREC) of Griffith University. In addition, informed consent was obtained for any experimentation.

Acknowledgements

This work was performed in part at the Queensland node of the Australian National Fabrication Facility, a company established under the National Collaborative Research Infrastructure Strategy to provide nano and micro-fabrication facilities for Australia's researchers. This work has been partially supported by the Griffith University's New Researcher Grants and Australian Research Council grant LP150100153. We would like to thank Dr Peter Woodfield for his comments and suggestions.

References

1 Y. Cui and C. M. Lieber, *Science*, 2001, **291**, 851.
2 T. Dinh, D. V. Dao, H.-P. Phan, L. Wang, A. Qamar, N.-T. Nguyen, P. Tanner and M. Rybachuk, *Appl. Phys. Express*, 2015, **8**, 061303.
3 M. Schulz, *Nature*, 1999, **399**, 729.
4 T. Dinh, H. P. Phan, T. Kozeki, A. Qamar, T. Fujii, T. Namazu, N. T. Nguyen and D. V. Dao, *Mater. Lett.*, 2016, **177**, 80.
5 H. P. Phan, D. V. Dao, K. Nakamura, S. Dimitrijev and N. T. Nguyen, *J. Microelectromech. Syst.*, 2015, **24**, 1663.
6 T. Dinh, H.-P. Phan, T. Kozeki, A. Qamar, T. Namazu, N.-T. Nguyen and D. V. Dao, *RSC Adv.*, 2015, **5**, 106083.
7 S. Choi, H. Lee, R. Ghaffari, T. Hyeon and D. H. Kim, *Adv. Mater.*, 2016, **28**, 4203.
8 S. Hong, H. Lee, J. Lee, J. Kwon, S. Han, Y. D. Suh, H. Cho, J. Shin, J. Yeo and S. H. Ko, *Adv. Mater.*, 2015, **27**, 4744.
9 K. Takei, W. Honda, S. Harada, T. Arie and S. Akita, *Adv. Healthcare Mater.*, 2015, **4**, 487.
10 P. Jiang, S. Zha and R. Zhu, *Sensors*, 2015, **15**, 31738.
11 M. Folke, L. Cernerud, M. Ekstrom and B. Hok, *Med. Biol. Eng. Comput.*, 2003, **41**, 377–383.
12 H. Sturm and W. Lang, *Sens. Actuators, A*, 2013, **195**, 113–122.
13 T. Dinh, H.-P. Phan, A. Qamar, N.-T. Nguyen and D. V. Dao, *RSC Adv.*, 2016, **6**, 77267.
14 B. H. Nguyen and V. H. Nguyen, *Adv. Nat. Sci.: Nanosci. Nanotechnol.*, 2016, **7**, 023002.
15 X. Liu, C. Liu, C. V. Catapano, L. Peng, J. Zhou and P. Rocchi, *Biotechnol. Adv.*, 2014, **32**, 844.
16 T. Q. Trung and N. E. Lee, *Adv. Mater.*, 2016, **28**, 4338.
17 T. Q. Trung, S. Ramasundaram, B. U. Hwang and N. E. Lee, *Adv. Mater.*, 2016, **28**, 502.
18 Y. Khan, A. E. Ostfeld, C. M. Lochner, A. Pierre and A. C. Arias, *Adv. Mater.*, 2015, **28**, 4373.
19 D. H. Kim, S. Wang, H. Keum, R. Ghaffari, Y. S. Kim, H. Tao, B. Panilaitis, M. Li, Z. Kang and F. Omenetto, *Small*, 2012, **8**, 3263.
20 J. Yang, D. Wei, L. Tang, X. Song, W. Luo, J. Chu, T. Gao, H. Shi and C. Du, *RSC Adv.*, 2015, **5**, 25609.
21 J. Kim, M. Lee, H. J. Shim, R. Ghaffari, H. R. Cho, D. Son, Y. H. Jung, M. Soh, C. Choi and S. Jung, *Nat. Commun.*, 2014, **5**, 5747.
22 W. Zeng, L. Shu, Q. Li, S. Chen, F. Wang and X. M. Tao, *Adv. Mater.*, 2014, **26**, 5310.
23 V. Zardetto, T. M. Brown, A. Reale and A. Di Carlo, *J. Polym. Sci., Part B: Polym. Phys.*, 2011, **49**, 638.
24 D. Zhang, K. Ryu, X. Liu, E. Polikarpov, J. Ly, M. E. Tompson and C. Zhou, *Nano Lett.*, 2006, **6**, 1880.
25 E. Artukovic, M. Kaempgen, D. S. Hecht, S. Roth and G. Grüner, *Nano Lett.*, 2005, **5**, 757.
26 N. K. Chang, C. C. Su and S. H. Chang, *Appl. Phys. Lett.*, 2008, **92**, 063501.
27 S. Park, M. Vosguerichian and Z. Bao, *Nanoscale*, 2013, **5**, 1727.
28 C. D. Tran, W. Humphries, S. M. Smith, C. Huynh and S. Lucas, *Carbon*, 2009, **47**, 2662.
29 K. Liu, Y. Sun, R. Zhou, H. Zhu, J. Wang, L. Liu, S. Fan and K. Jiang, *Nanotechnology*, 2009, **21**, 045708.
30 K. Liu, Y. Sun, X. Lin, R. Zhou, J. Wang, S. Fan and K. Jiang, *ACS Nano*, 2010, **4**, 5827.
31 W. Lu, M. Zu, J. H. Byun, B. S. Kim and T. W. Chou, *Adv. Mater.*, 2012, **24**, 1805.
32 Q. Cao, H. S. Kim, N. Pimparkar, J. P. Kulkarni, C. Wang, M. Shim, K. Roy, M. A. Alam and J. A. Rogers, *Nature*, 2008, **454**, 495.
33 Y. Zhou, L. Hu and G. Grüner, *Appl. Phys. Lett.*, 2006, **88**, 123109.
34 T. Dinh, H. P. Phan, D. V. Dao, P. Woodfield, A. Qamar and N. T. Nguyen, *J. Mater. Chem. C*, 2015, **3**, 8776.
35 K. Cattanach, R. D. Kulkarni, M. Kozlov and S. K. Manohar, *Nanotechnology*, 2006, **17**, 4123.
36 T. Sekitani, H. Nakajima, H. Maeda, T. Fukushima, T. Aida, K. Hata and T. Someya, *Nat. Mater.*, 2009, **8**, 494.
37 Y. J. Kang, S. J. Chun, S. S. Lee, B. Y. Kim, J. H. Kim, H. Chung, S. Y. Lee and W. Kim, *ACS Nano*, 2012, **6**, 6400.
38 H. Zhao, Y. Zhang, P. D. Bradford, Q. Zhou, Q. Jia, F. G. Yuan and Y. Zhu, *Nanotechnology*, 2010, **21**, 305502.
39 J. L. Abot, T. Alosh and K. Belay, *Carbon*, 2014, **70**, 95–102.
40 J. Zhou, G. Yan, Y. Zhu, Z. Xiao and J. Fan, *In IEEE 18th International Conference on Micro Electro Mechanical Systems*, 2005, pp. 363–366.
41 V. T. Dau, D. V. Dao and S. Sugiyama, *Smart Mater. Struct.*, 2007, **16**, 2308.
42 S. O. Kasap, *Semiconductor, Principles of Electronic Materials and Devices*, McGraw-Hill, New York, NY, 2006, p. 373.
43 S. S. Li and W. R. Thurber, *Solid-State Electron.*, 1977, **20**, 609–616.
44 C. Yu, Z. Wang, H. Yu and H. Jiang, *Appl. Phys. Lett.*, 2009, **95**, 141912.
45 J. Courbat, Y. B. Kim, D. Briand and N. F. De Rooij, *In Solid-State Sensors, Actuators and Microsystems Conference (TRANSDUCERS), 16th International, IEEE*, 2011, pp. 1356–1359.

46 A. Di Bartolomeo, M. Sarno, F. Giubileo, C. Altavilla, L. Iemmo, S. Piano, F. Bobba, M. Longobardi, A. Scarfato, D. Sannino and A. M. Cucolo, *J. Appl. Phys.*, 2009, **105**, 064518.
47 C. L. Kane, E. J. Mele, R. S. Lee, J. E. Fischer, P. Petit, H. Dai, A. Thess, R. E. Smalley, A. R. M. Verschueren, S. J. Tans and C. Dekker, *EPL*, 1998, **41**, 683.
48 K. F. Jensen, *Chem. Eng. Sci.*, 2001, **56**, 293.
49 J. Che, T. Cagin and W. A. Goddard III, *Nanotechnology*, 2000, **11**, 65.
50 E. D. Minot, Y. Yaish, V. Sazonova, J. Y. Park, M. Brink and P. L. McEuen, *Phys. Rev. Lett.*, 2003, **90**, 156401.
51 S. T. Hung, S. C. Wong and W. Fang, *Sens. Actuators, A*, 2000, **84**, 70.
52 F. Mailly, A. Giani, R. Bonnot, P. Temple-Boyer, F. Pascal-Delannoy, A. Foucaran and A. Boyer, *Sens. Actuators, A*, 2001, **94**, 32.
53 T. Neda, K. Nakamura and T. Takumi, *Sens. Actuators, A*, 1996, **54**, 626.
54 R. G. Johnson and R. E. Higashi, *Sens. Actuators*, 1987, **11**, 63.
55 M. Petrovic, J. Petrovic, A. Danicic, M. Vukcevic, B. Bojovic, L. Hazievski, T. Allsop, G. Lloyd and D. Webb, *Biomed. Opt. Express*, 2014, **5**, 1136.
56 P. Jiang, S. Zhao and R. Zhu, *Sensors*, 2015, **15**, 31738.

